Exponentially Improved Dispersive Qubit Readout with Squeezed Light

Wei Qin,[1,2,6,*] Adam Miranowicz,[2,3] and Franco Nori[2,4,5]

[1]Center for Joint Quantum Studies and Department of Physics, School of Science, Tianjin University, Tianjin 300350, China
[2]Theoretical Quantum Physics Laboratory, Cluster for Pioneering Research, RIKEN, Wako shi, Saitama 351-0198, Japan
[3]Institute of Spintronics and Quantum Information, Faculty of Physics, Adam Mickiewicz University, 61-614 Poznań, Poland
[4]Center for Quantum Computing, RIKEN, Wako shi, Saitama 351-0198, Japan
[5]Department of Physics, The University of Michigan, Ann Arbor, Michigan 48109-1040, USA
[6]Tianjin Key Laboratory of Low Dimensional Materials Physics and Preparing Technology, Tianjin University, Tianjin 300350, China

(Received 19 February 2024; accepted 16 September 2024; published 5 December 2024)

It has been a long-standing goal to improve dispersive qubit readout with squeezed light. However, injected external squeezing (IES) *cannot* enable a practically interesting increase in the signal-to-noise ratio (SNR), and simultaneously, the increase of the SNR due to the use of intracavity squeezing (ICS) is even *negligible*. Here, we *counterintuitively* demonstrate that using IES and ICS together can lead to an *exponential* improvement of the SNR for any measurement time, corresponding to a measurement error reduced typically by many orders of magnitude. More remarkably, we find that in a short-time measurement, the SNR is even improved exponentially with *twice* the squeezing parameter. As a result, we predict a fast and high-fidelity readout. This work offers a promising path toward exploring squeezed light for dispersive qubit readout, with immediate applications in quantum error correction and fault-tolerant quantum computation.

DOI: 10.1103/PhysRevLett.133.233605

Introduction—Squeezed light is a powerful resource in modern quantum technologies [1–3]. It has been widely used for various applications, including quantum key distribution [4–7], mechanical cooling [8–11], light-matter interaction enhancement [12–18], and even quantum advantage demonstration [19–21]. In particular, such nonclassical light plays a central role in high-precision quantum measurements [22,23], e.g., gravitational-wave detection [24–26], optomechanical motion sensing [27,28], and longitudinal qubit readout [29,30]. Despite these achievements, how to utilize squeezed light to improve dispersive qubit readout (DQR) still remains an unresolved challenge [31–35].

DQR [36–41], as a common nondemolition readout, forms a crucial component of quantum error correction [42–44] and fault-tolerant quantum computation [45,46]. In the readout, a qubit to be measured is dispersively coupled to a cavity working as the pointer, so that a qubit-state-dependent cavity resonance shift is induced and then measured by homodyne detection. Usually, this readout is required to be fast and of high fidelity, and exploiting squeezed states of light to improve such a readout is, therefore, highly desirable [35]. However, it has already been shown that injected external squeezing (IES) *cannot* significantly improve the signal-to-noise ratio (SNR) in an experimentally feasible way [32,47,50]. The reason is attributed to a qubit-state-dependent rotation of squeezing and, thus, an increase in the overlap of the two pointer states [see Fig. 1(a)]. Furthermore, one might suggest the use of intracavity squeezing (ICS) generated, e.g., by a two-photon driving. However, in this case, the resulting improvement in the SNR is even *negligible* [47]. In addition to a detrimental rotation of squeezing, as in the case of IES, the reason is also related to the degree of squeezing that increases gradually from zero with the measurement time, as a result even causing a larger overlap of the pointer states [see Fig. 1(b)]. Hence, one can conclude that standard DQR *cannot* benefit well from the *separate* use of IES and ICS.

In this Letter, we *counterintuitively* demonstrate that when IES and ICS are applied simultaneously, the readout SNR can have an *exponential* improvement for any measurement time. In our approach, the qubit-state information is mapped onto a Bogoliubov mode of the cavity, rather than the bare cavity mode as usual. This ensures a strong and measurement-time-independent degree of squeezing, and also avoids the qubit-state-dependent rotation of squeezing. Thus in sharp contrast to the case of using IES or ICS alone, the overlap of the pointer states is exponentially decreased [see Fig. 1(c)]. Note that a heuristic approach that can exponentially improve the SNR of DQR has been previously proposed, based on a quantum-mechanics-free subsystem [32]. But it needs to inject two-mode squeezed light into two coupled cavities, and measure a pair of readout modes. In contrast, our approach relies on a single cavity and single-mode squeezed light,

*Contact author: qin.wei@tju.edu.cn

 © 2024 American Physical Society

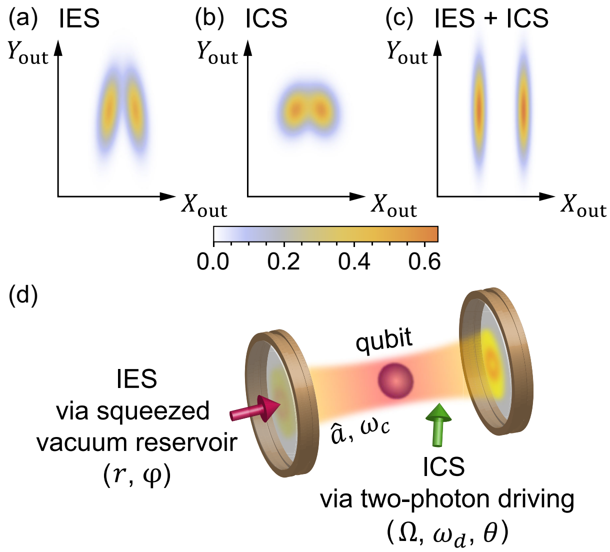

FIG. 1. (a)–(c) Phase-space representation of DQR with IES, ICS, and these two simultaneously. The separate use of IES and ICS cannot enable a significant improvement of practical interest in the SNR, but their simultaneous use can. (d) Schematic of DQR with both IES and ICS. The qubit is dispersively coupled to the cavity mode $\hat{a}$ of frequency ω_c. A squeezed vacuum reservoir (squeezing parameter r, reference phase φ) provides IES for the cavity, while a two-photon driving (amplitude Ω, frequency ω_d, phase θ) is used to generate ICS.

therefore more suitable for the standard readout. More surprisingly, we find that the resulting SNR can scale as e^{2r} for short-time measurements, rather than e^{r} as given in Ref. [32], indicating a fast and high-fidelity readout. Here, r refers to the squeezing parameter. Such a giant improvement arises due to two aspects, one from antisqueezed vacuum fluctuations, which amplify the qubit-cavity dispersive coupling and, thus, the signal separation (i.e., the pointer-state separation), and the other from squeezed vacuum fluctuations, which reduce the measurement noise.

Physical model—The key idea underlying our proposal is shown in Fig. 1(d). The qubit is coupled to the cavity via a detuned interaction $\hat{H}_{\rm int} = g(\hat{a}^\dagger\hat{\sigma}_- + \hat{a}\hat{\sigma}_+)$, with a strength g. Here, $\hat{a}$ ($\hat{a}^\dagger$) is the annihilation (creation) operator of the cavity, and $\hat{\sigma}_-$ ($\hat{\sigma}_+$) is the lowering (raising) operator of the qubit. We assume that a squeezed vacuum reservoir, with a squeezing parameter r and a reference phase φ, is injected into the cavity as IES [10,51–54]. To generate ICS, the cavity is further assumed to be pumped by a two-photon driving of amplitude Ω, frequency ω_d, and phase θ. The system Hamiltonian in a frame rotating at ω_d is

$$\hat{H} = \Delta_c\hat{a}^\dagger\hat{a} + \frac{1}{2}\Delta_q\hat{\sigma}_z + \hat{H}_{\rm int} + \Omega(e^{i\theta}\hat{a}^{\dagger 2} + e^{-i\theta}\hat{a}^2), \qquad (1)$$

where $\hat{\sigma}_z$ is a qubit Pauli operator, $\Delta_c = \omega_c - \omega_d/2$, and $\Delta_q = \omega_q - \omega_d/2$. Here, ω_c is the cavity frequency, and ω_q is the qubit transition frequency. The Langevin equation of motion for the cavity mode $\hat{a}$ is, therefore, given by

$$\dot{\hat{a}}(t) = -i(\Delta_c - i\kappa/2)\hat{a} - i2\Omega e^{i\theta}\hat{a}^\dagger - ig\hat{\sigma}_- - \sqrt{\kappa}\hat{a}_{\rm in}(t), \qquad (2)$$

where κ is the cavity-photon loss rate, and $\hat{a}_{\rm in}(t)$ represents the cavity input field. The correlations for the input-noise operator $\hat{\mathcal{A}}_{\rm in}(t) = \hat{a}_{\rm in}(t) - \langle\hat{a}_{\rm in}(t)\rangle$ are $\langle\hat{\mathcal{A}}_{\rm in}(t)\hat{\mathcal{A}}_{\rm in}^\dagger(t')\rangle = \cosh^2(r)\delta(t-t')$ and $\langle\hat{\mathcal{A}}_{\rm in}(t)\hat{\mathcal{A}}_{\rm in}(t')\rangle = \frac{1}{2}e^{i\varphi}\sinh(2r)\delta(t-t')$, due to IES.

We below consider the case of $\Delta_c \neq 0$, and introduce a Bogoliubov mode, $\hat{\beta} = \cosh(r_c)\hat{a} + e^{i\theta}\sinh(r_c)\hat{a}^\dagger$. Here, $\tanh(2r_c) = 2\Omega/\Delta_c$. According to Eq. (2), the evolution of the mode $\hat{\beta}$ follows

$$\dot{\hat{\beta}}(t) = -i(\omega_{\rm sq} - i\kappa/2)\hat{\beta} - ig\hat{S}_- - \sqrt{\kappa}\hat{\beta}_{\rm in}(t), \qquad (3)$$

where $\omega_{\rm sq} = \sqrt{\Delta_c^2 - 4\Omega^2}$ is the resonance frequency of the mode $\hat{\beta}$, $\hat{S}_- = \cosh(r_c)\hat{\sigma}_- - e^{i\theta}\sinh(r_c)\hat{\sigma}_+$, and $\hat{\beta}_{\rm in}(t) = \cosh(r_c)\hat{a}_{\rm in}(t) + e^{i\theta}\sinh(r_c)\hat{a}_{\rm in}^\dagger(t)$. Upon choosing $r_c = r$ and $\theta - \varphi = \pi$, the correlations for the noise operator $\hat{\mathcal{B}}_{\rm in}(t) = \hat{\beta}_{\rm in}(t) - \langle\hat{\beta}_{\rm in}(t)\rangle$ are [47]

$$\langle\hat{\mathcal{B}}_{\rm in}(t)\hat{\mathcal{B}}_{\rm in}^\dagger(t')\rangle = \delta(t-t'), \qquad \langle\hat{\mathcal{B}}_{\rm in}(t)\hat{\mathcal{B}}_{\rm in}(t')\rangle = 0. \qquad (4)$$

Therefore, $\hat{\mathcal{B}}_{\rm in}(t)$ can be now thought of as the vacuum noise. Note that similar techniques of noise elimination have been used, e.g., to enhance light-matter interactions [12–14,55–59], prepare nonclassical states [60], generate squeezed lasing [61], and induce optical nonreciprocity [62]. However, these studies are based on the amplified fluctuations in an antisqueezed quadrature. To improve DQR, here we also exploit the reduced fluctuations in a squeezed quadrature, and as an overall result, we achieve an improved SNR scaling as e^{2r} in a short-time measurement (see below).

Furthermore, we assume $(\Delta_q + \omega_{\rm sq}) \gg g\cosh(r)$, and make a dispersive approximation [63]. The effective dynamics of the system can be described by

$$\dot{\hat{\beta}}(t) = -i(\omega_{\rm sq} + \chi_{\rm sq}\hat{\sigma}_z - i\kappa/2)\hat{\beta} - \sqrt{\kappa}\hat{\beta}_{\rm in}(t). \qquad (5)$$

Here, the $\hat{\sigma}_z$ term corresponds to a dispersive coupling, $\hat{V}_{\rm sq} = \chi_{\rm sq}\hat{\beta}^\dagger\hat{\beta}\hat{\sigma}_z$, of the qubit and the mode $\hat{\beta}$ [47], with a strength

$$\chi_{\rm sq} = \chi\{\cosh(r) + \sinh^2(r)/[\cosh(r) + 2\omega_{\rm sq}\epsilon/g]\}, \qquad (6)$$

where $\chi = g\epsilon$ with $\epsilon = g\cosh(r)/(\Delta_q - \omega_{\rm sq})$. The dispersive coupling of the qubit and the bare mode $\hat{a}$, used for standard DQR, is usually obtained by applying a dispersive approximation to the detuned interaction $\hat{H}_{\rm int}$, and is given by $\hat{V}_0 = \chi_0\hat{a}^\dagger\hat{a}\hat{\sigma}_z$, where $\chi_0 = g\epsilon_0$ with $\epsilon_0 = g/(\omega_q - \omega_c)$.

It is seen that in our readout, the qubit-state information is mapped onto the Bogoliubov mode $\hat{a}_{\rm sq}$, rather than the bare mode $\hat{a}$ as in the standard readout; i.e., the qubit shifts the resonance of the mode $\hat{a}_{\rm sq}$, rather than the mode $\hat{a}$.

Note that the parameters ϵ_0 and ϵ determine the validity or accuracy of the dispersive approximations applied for $\hat{V}_0$ and $\hat{V}_{\rm sq}$, respectively. To compare $\hat{V}_0$ and $\hat{V}_{\rm sq}$ fairly, they need to have the same validity (i.e., $\epsilon_0 = \epsilon$) and, in such a case, χ can be regarded as the dispersive coupling strength χ_0 (i.e., $\chi = \chi_0$) (see [47] for more details). Consequently, as plotted in Fig. 2(a), $\chi_{\rm sq}$ becomes significantly enhanced by squeezing, compared to χ_0 (i.e., χ). Particularly, for $\epsilon \ll 1$, we obtain an exponential enhancement,

$$\chi_{\rm sq} \simeq \chi \exp(r), \tag{7}$$

which, physically, originates from the amplification of the qubit-cavity coupling from g to $\simeq g e^r$ by the antisqueezing of vacuum fluctuations. As demonstrated below, such an enhancement can exponentially increase the signal separation and, thus, the readout SNR for short-time measurements.

Exponentially enhanced DQR—The output quadrature measured via homodyne detection is $\hat{\mathcal{Z}}_{\rm out}(t) = \hat{a}_{\rm out}(t)e^{-i\phi_h} + \hat{a}^\dagger_{\rm out}(t)e^{i\phi_h}$. Here, $\hat{a}_{\rm out}(t) = \cosh(r)\hat{\beta}_{\rm out}(t) - e^{i\theta}\sinh(r)\hat{\beta}^\dagger_{\rm out}(t)$, where $\hat{\beta}_{\rm out}(t) = \hat{\beta}_{\rm in}(t) + \sqrt{\kappa}\hat{\beta}$, represents the cavity output field, and ϕ_h is the measurement angle. The SNR, an essential parameter to quantify homodyne detection, is defined as

$$\mathrm{SNR} = |\langle \hat{M}\rangle_\uparrow - \langle \hat{M}\rangle_\downarrow|(\langle \hat{M}_N^2\rangle_\uparrow + \langle \hat{M}_N^2\rangle_\downarrow)^{-1/2}. \tag{8}$$

Here, $\hat{M} = \sqrt{\kappa}\int_0^\tau dt \hat{\mathcal{Z}}_{\rm out}(t)$ is the measurement operator with a measurement time τ, $\hat{M}_N = \hat{M} - \langle \hat{M}\rangle$ is the fluctuation-noise operator, and $\{\downarrow, \uparrow\}$ labels the qubit state. Note that although our proposal is based on the coupling $\hat{V}_{\rm sq}$ in the squeezed frame, the SNR in Eq. (8) is still given in the original lab frame as usual. Therefore, the SNR improvement mentioned below is measurable.

We now consider the measurement noise $\langle \hat{M}_N^2\rangle$. The cavity output-noise operator, $\hat{\mathcal{A}}_{\rm out}(t) = \hat{a}_{\rm out}(t) - \langle \hat{a}_{\rm out}(t)\rangle$, can be expressed as $\hat{\mathcal{A}}_{\rm out}(t) = \cosh(r)\hat{\mathcal{B}}_{\rm out}(t) - e^{i\theta}\sinh(r)\hat{\mathcal{B}}^\dagger_{\rm out}(t)$. Here, $\hat{\mathcal{B}}_{\rm out}(t) = \hat{\beta}_{\rm out}(t) - \langle \hat{\beta}_{\rm out}(t)\rangle$. From Eqs. (4) and (5), we find $\langle \hat{\mathcal{B}}_{\rm out}(t)\hat{\mathcal{B}}^\dagger_{\rm out}(t')\rangle = \delta(t-t')$ and $\langle \hat{\mathcal{B}}_{\rm out}(t)\hat{\mathcal{B}}_{\rm out}(t')\rangle = 0$. It follows that

$$\langle \hat{\mathcal{A}}_{\rm out}(t)\hat{\mathcal{A}}^\dagger_{\rm out}(t')\rangle = \cosh^2(r)\delta(t-t'), \tag{9}$$

$$\langle \hat{\mathcal{A}}_{\rm out}(t)\hat{\mathcal{A}}_{\rm out}(t')\rangle = -\frac{1}{2}e^{i\theta}\sinh(2r)\delta(t-t'), \tag{10}$$

and then that

$$\langle \hat{M}_N^2\rangle = \kappa\tau[\cosh(2r) - \cos(2\phi_h - \theta)\sinh(2r)]. \tag{11}$$

Clearly, $\langle \hat{M}_N^2\rangle$ is qubit-state independent for any measurement time, in stark contrast to the case of using IES or ICS alone [see Figs. 1(a) and 1(b)]. Furthermore, choosing $2\phi_h = \theta$ gives

$$\langle \hat{M}_N^2\rangle = \kappa\tau\exp(-2r), \tag{12}$$

indicating an exponential suppression of the measurement noise for any measurement time.

Consider a coherent measurement tone, $\langle \hat{a}_{\rm in}(t)\rangle = \alpha_{\rm in}e^{i\phi_{\rm in}}$. Since the signal separation is proportional to $|\langle \hat{\beta}_{\rm in}(t)\rangle|$ [47], we therefore maximize $|\langle \hat{\beta}_{\rm in}(t)\rangle|$ by assuming $2\phi_{\rm in} = \theta$, yielding $\langle \hat{\beta}_{\rm in}(t)\rangle = \alpha_{\rm in}e^r e^{i\phi_{\rm in}}$. Note that in the optimal case of using IES or ICS alone, the signal separation perpendicular to the measurement direction, labeled $|\langle \hat{M}\rangle_\uparrow - \langle \hat{M}\rangle_\downarrow|_\perp$, always vanishes [47], but not in the case of their simultaneous use. Thus, for comparison, we require $|\langle \hat{M}\rangle_\uparrow - \langle \hat{M}\rangle_\downarrow|_\perp = 0$ in our proposal, although reducing the SNR slightly. For a given measurement time, this requirement can be exactly satisfied by tuning $\omega_{\rm sq}$, as depicted in the inset of Fig. 2(a).

Before presenting numerical simulations, let us first discuss the two limits, i.e., $\kappa\tau \to 0$ and ∞. In the short-time limit $\kappa\tau \to 0$, the SNR is given by [47]

$$\mathrm{SNR} \simeq 0.81\exp(2r)\mathrm{SNR}_{\rm std}, \tag{13}$$

where $\mathrm{SNR}_{\rm std}$ refers to the SNR of the standard readout with no squeezing. Surprisingly, we find that the SNR is improved exponentially with $2r$. There are two reasons for this. First, the measurement noise is exponentially reduced, as seen in Eq. (12). Second, the signal separation, $\simeq 0.27\alpha_{\rm in}\kappa^{-1/2}\tan(\psi_{\rm sq})(\kappa\tau)^3$, with $\tan(\psi_{\rm sq}) = 2\chi_{\rm sq}/\kappa$, is increased by a factor e^r, due to the enhanced $\chi_{\rm sq}$ as given in Eq. (7). Instead, in the long-time limit $\kappa\tau \to \infty$, the signal separation, $\simeq 4\alpha_{\rm in}\kappa^{-1/2}\sin(\psi_{\rm sq})\kappa\tau$, is not changed significantly by $\chi_{\rm sq}$ or r; thus, we also have an exponential improvement but with r, i.e.,

$$\mathrm{SNR} \simeq \frac{\sin(\psi_{\rm sq})}{\sin(2\psi)}\exp(r)\mathrm{SNR}_{\rm std}. \tag{14}$$

In Figs. 2(b) and 2(c), we plot the SNR and the measurement error, $\delta_m = 1 - \mathcal{F}_m$, for DQR using IES, ICS, and both of them. Here, $\mathcal{F}_m = \frac{1}{2}[1 + \mathrm{erf}(\mathrm{SNR}/2)]$ refers to the measurement fidelity. Note that in the case of ICS, we have defined $r = \ln[(\kappa + 4\Omega)/(\kappa - 4\Omega)]$, which is the squeezing parameter of the cavity output field in the absence of the qubit. Clearly, for any measurement time, our approach can enable at least an exponential improvement with r, compared to the other approaches. Assuming realistic parameters of $\alpha_{\rm in}/\sqrt{\kappa} = 1$, $\chi = \kappa/2$, and $\kappa = 2\pi \times 5$ MHz, a typical measurement time of $\tau = 1/\kappa \simeq 32$ ns results in

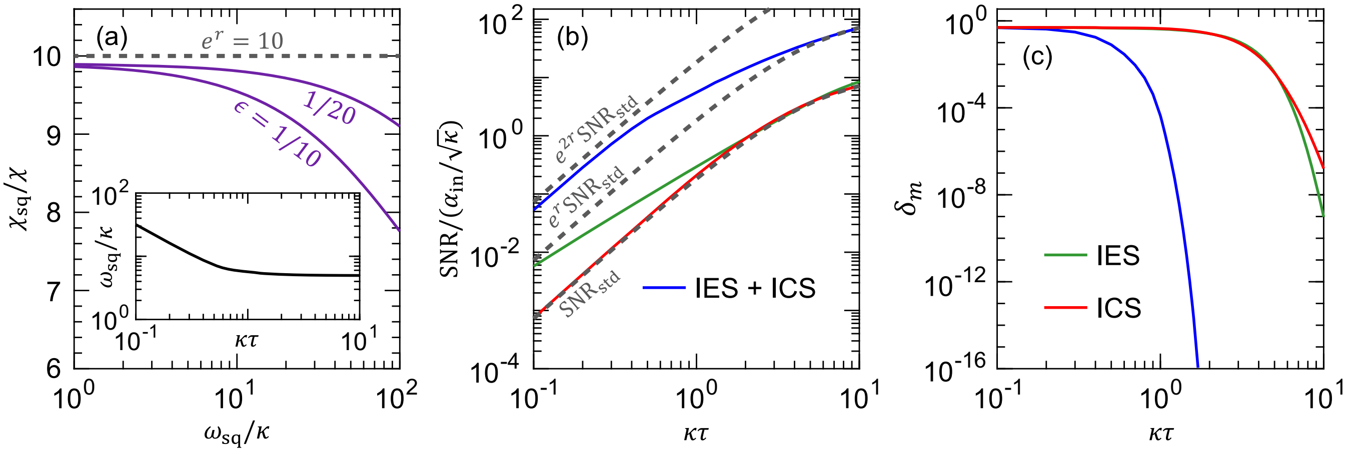

FIG. 2. (a) Dispersive coupling enhancement, i.e, $\chi_{\rm sq}/\chi$, versus the effective cavity frequency $\omega_{\rm sq}$, for $e^r = 10$ and $\epsilon = 1/10, 1/20$. It is clearly seen that a significant and even an exponential enhancement can be obtained. Inset: $\omega_{\rm sq}$ required to achieve $|\langle \hat{M}\rangle_\uparrow - \langle \hat{M}\rangle_\downarrow|_\perp = 0$ versus the measurement time $\kappa\tau$. (b) SNR and (c) measurement error δ_m versus $\kappa\tau$. The three dashed curves in (b) represent $\mathrm{SNR}_{\rm std}$ (i.e., the SNR of the standard readout with no squeezing), $e^r\mathrm{SNR}_{\rm std}$, and $e^{2r}\mathrm{SNR}_{\rm std}$, respectively. In the cases of separately using IES (green) and ICS (red), the optimization has been made for the squeezing parameter r in the range $1 \le e^r \le 10$, while we have set $\epsilon = 1/20$ and $e^r = 10$ in the readout of using both IES and ICS (blue). In (c), $\alpha_{\rm in}/\sqrt{\kappa} = 1$, and in all plots, $\chi = \kappa/2$.

$\mathrm{SNR} \simeq 5.5$ for $e^r = 10$, corresponding to a measurement error of $\delta_m \simeq 4.4 \times 10^{-5}$. In stark contrast, we find $\mathrm{SNR} \simeq 0.18$, 0.29, and 0.21 for the readout with no squeezing, IES, and ICS, respectively. The corresponding measurement errors are $\delta_m \simeq 0.45$, 0.42, and 0.44, all approximately 6 orders of magnitude larger than what is obtained using our approach. Indeed, as analyzed in detail in Ref. [47], the use of IES or ICS alone cannot enable a significant SNR increase of practical interest.

Fast DQR—Standard DQR, although simple, cannot be improved arbitrarily by simply increasing the measurement-tone amplitude. The reason is because the cavity-photon number n typically needs to be kept well below the critical photon number $n_c = 1/4\epsilon^2$, to avoid the breakdown of the dispersive approximation [64]. This makes the readout very slow. However, as mentioned above, the SNR obtained using our approach is improved by a factor e^{2r} in the short-time measurement, implying that a fast and high-fidelity readout can be achieved.

In Figs. 3(a) and 3(b), we depict the measurement-tone amplitude $\alpha_{\rm in}$ and the cavity-photon number n, needed to reach $\mathrm{SNR} = 1$, for the three cases of using IES, ICS, and both of them. In our approach, the dispersive approximation is made for the mode $\hat{\beta}$, rather than the mode $\hat{a}$; therefore, the cavity-photon number, used to evaluate the validity of this approximation, is $n = \langle \hat{\beta}^\dagger(t)\hat{\beta}(t)\rangle$ [47]. Clearly, our approach enables a much shorter measurement time. For example, we use a measurement tone of $\alpha_{\rm in}/\sqrt{\kappa} \simeq 3.5$, corresponding to $n \simeq 29$ cavity photons, to have $\mathrm{SNR} = 1$ for a short measurement time of $\tau = 0.2/\kappa \simeq 6.4$ ns. Here, $\kappa = 2\pi \times 5$ MHz. However, to reach the same SNR at the same measurement time, the approaches based on IES and ICS need the much stronger measurement tones of $\alpha_{\rm in}/\sqrt{\kappa} \simeq 52$ and $\simeq 239$, respectively, resulting in $n \simeq 107$ and $\simeq 2238$ cavity photons, both higher than the critical photon number $n_c = 100$. Note that, here, the standard readout of no squeezing has almost the same results as in the case of ICS.

Experimental feasibility—So far, we have discussed an ideal model where $r_c = r$ and $\theta - \varphi = \pi$. However, there are always some parameter mismatches in realistic experiments, such that $r_c = r + \delta_r$, and $\theta - \varphi = \pi + \delta_p$, where δ_r and δ_p are the squeezing-degree and -direction mismatches, respectively. A detailed derivation of the SNR in such an imperfect case is given in Ref. [47]. We plot in Fig. 4 the SNR in the presence of these parameter mismatches. It is

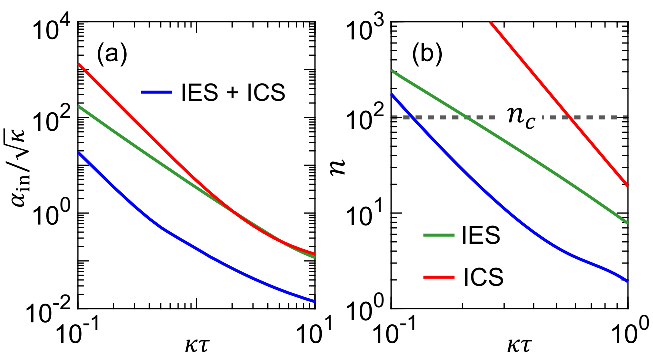

FIG. 3. (a) Measurement-tone amplitude $\alpha_{\rm in}/\sqrt{\kappa}$ and (b) cavity-photon number n, required to achieve $\mathrm{SNR} = 1$, versus $\kappa\tau$. In our approach, the photon number n depends on the qubit state, and we depict the maximum values here. The horizontal dashed line indicates the critical photon number $n_c = 100$. It is seen that our approach can keep n well below n_c at a much smaller $\kappa\tau$, compared to the other approaches. In both plots, the parameters are chosen as in Fig. 2(b).

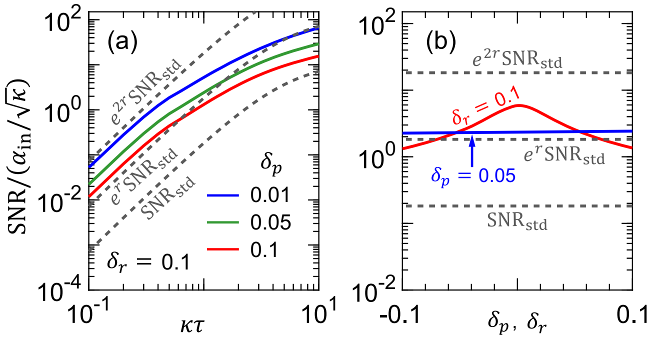

FIG. 4. SNR versus $\kappa\tau$ for some fixed parameter mismatches in (a), and versus the parameter mismatch for $\kappa\tau = 1$ in (b). We assumed $\delta_p = 0.1, 0.05, 0.01$, and $\delta_r = 0.1$ (see Ref. [47] for the $\delta_r = 0.01$ case) in (a). In (b), the red and blue curves show the robustness against the squeezing-direction mismatch δ_p for $\delta_r = 0.1$ and the squeezing-degree mismatch δ_r for $\delta_p = 0.05$, respectively. In both plots, other parameters and what the three dashed curves represent are the same as in Fig. 2(b).

seen from Fig. 4(a) that the exponential improvement in the SNR remains even in the presence of finite parameter mismatches. We also find from Fig. 4(b) that the SNR is sensitive to the squeezing-direction mismatch but, interestingly, is very robust against the squeezing-degree mismatch. Clearly, an SNR improvement nearly exponential can still be achieved at a measurement time $\tau \sim 1/\kappa$, even for large mismatches of $\delta_p = 0.1$ and $\delta_r = 0.1$; e.g., $\mathrm{SNR} \simeq 0.72 \exp(r)\mathrm{SNR}_{\mathrm{std}}$, at $\tau = 1/\kappa$. Moreover, our readout proposal is valid for a wide range of physical systems. Particularly, in superconducting quantum circuits, IES and ICS can be implemented using Josephson parametric amplifiers [10,51,65]. Hence, our proposal is experimentally feasible.

Conclusions—We have presented a method of simultaneously using IES and ICS to improve DQR. This method can enable at least an exponential improvement of the SNR with the squeezing parameter. In particular, the short-time SNR is improved exponentially with twice the squeezing parameter, therefore leading to a fast and high-fidelity readout. In stark contrast, using IES or ICS alone cannot make a significant and practically useful increase in the SNR. Our proposal opens a promising perspective for the use of squeezing, and could further stimulate more applications of squeezing for modern quantum technologies.

Note added—While completing this manuscript, we became aware of [66], which also discusses the simultaneous use of IES and ICS for DQR. However, that work does not take full advantage of squeezing, and shows a completely different result, i.e., a modest (not an exponential as predicted in our present work) improvement in the SNR.

Acknowledgments—W. Q. acknowledges support of the National Natural Science Foundation of China (NSFC) via Grant No. 0401260012. A. M. is supported by the Polish National Science Centre (NCN) under the Maestro Grant No. DEC-2019/34/A/ST2/00081. F. N. is supported in part by: Nippon Telegraph and Telephone Corporation (NTT) Research, the Japan Science and Technology Agency (JST) [via the CREST Quantum Frontiers program Grant No. JPMJCR24I2, the Quantum Leap Flagship Program (Q-LEAP), and the Moonshot R&D Grant No. JPMJMS2061], and the Office of Naval Research (ONR) Global (via Grant No. N62909-23-1-2074).

[1] M. O. Scully and M. S. Zubairy, *Quantum Optics* (Cambridge University Press, Cambridge, England, 1997).
[2] P. D. Drummond and Z. Ficek, *Quantum Squeezing* (Springer, Berlin, 2004).
[3] G. S. Agarwal, *Quantum Optics* (Cambridge University Press, Cambridge, England, 2013).
[4] T. C. Ralph, Continuous variable quantum cryptography, Phys. Rev. A **61**, 010303(R) (1999).
[5] N. J. Cerf, M. Lévy, and G. Van Assche, Quantum distribution of Gaussian keys using squeezed states, Phys. Rev. A **63**, 052311 (2001).
[6] L. S. Madsen, V. C. Usenko, M. Lassen, R. Filip, and U. L. Andersen, Continuous variable quantum key distribution with modulated entangled states, Nat. Commun. **3**, 1083 (2012).
[7] C. Peuntinger, B. Heim, C. R. Müller, C. Gabriel, C. Marquardt, and G. Leuchs, Distribution of squeezed states through an atmospheric channel, Phys. Rev. Lett. **113**, 060502 (2014).
[8] M. Asjad, S. Zippilli, and D. Vitali, Suppression of Stokes scattering and improved optomechanical cooling with squeezed light, Phys. Rev. A **94**, 051801(R) (2016).
[9] M. Asjad, N. E. Abari, S. Zippilli, and D. Vitali, Optomechanical cooling with intracavity squeezed light, Opt. Express **27**, 32427 (2019).
[10] J. B. Clark, F. Lecocq, R. W. Simmonds, J. Aumentado, and J. D. Teufel, Sideband cooling beyond the quantum backaction limit with squeezed light, Nature (London) **541**, 191 (2017).
[11] H.-K. Lau and A. A. Clerk, Ground-state cooling and high-fidelity quantum transduction via parametrically driven bad-cavity optomechanics, Phys. Rev. Lett. **124**, 103602 (2020).
[12] X.-Y. Lü, Y. Wu, J. R. Johansson, H. Jing, J. Zhang, and F. Nori, Squeezed optomechanics with phase-matched amplification and dissipation, Phys. Rev. Lett. **114**, 093602 (2015).
[13] W. Qin, A. Miranowicz, P.-B. Li, X.-Y. Lü, J. Q. You, and F. Nori, Exponentially enhanced light-matter interaction, cooperativities, and steady-state entanglement using parametric amplification, Phys. Rev. Lett. **120**, 093601 (2018).
[14] C. Leroux, L. C. G. Govia, and A. A. Clerk, Enhancing cavity quantum electrodynamics via antisqueezing: Synthetic ultrastrong coupling, Phys. Rev. Lett. **120**, 093602 (2018).
[15] W. Ge, B. C. Sawyer, J. W. Britton, K. Jacobs, J. J. Bollinger, and M. Foss-Feig, Trapped ion quantum

information processing with squeezed phonons, Phys. Rev. Lett. **122**, 030501 (2019).
[16] S. C. Burd, R. Srinivas, H. M. Knaack, W. Ge, A. C. Wilson, D. J. Wineland, D. Leibfried, J. J. Bollinger, D. T. C. Allcock, and D. H. Slichter, Quantum amplification of boson-mediated interactions, Nat. Phys. **17**, 898 (2021).
[17] M. Villiers, W. C. Smith, A. Petrescu, A. Borgognoni, M. Delbecq, A. Sarlette, M. Mirrahimi, P. Campagne-Ibarcq, T. Kontos, and Z. Leghtas, Dynamically enhancing qubit-photon interactions with antisqueezing, PRX Quantum **5**, 020306 (2024).
[18] W. Qin, A. F. Kockum, C. S. Muñoz, A. Miranowicz, and F. Nori, Quantum amplification and simulation of strong and ultrastrong coupling of light and matter, Phys. Rep. **1078**, 1 (2024).
[19] H.-S. Zhong *et al.*, Quantum computational advantage using photons, Science **370**, 1460 (2020).
[20] H.-S. Zhong *et al.*, Phase-programmable Gaussian boson sampling using stimulated squeezed light, Phys. Rev. Lett. **127**, 180502 (2021).
[21] L. S. Madsen *et al.*, Quantum computational advantage with a programmable photonic processor, Nature (London) **606**, 75 (2022).
[22] R. Schnabel, Squeezed states of light and their applications in laser interferometers, Phys. Rep. **684**, 1 (2017).
[23] B. J. Lawrie, P. D. Lett, A. M. Marino, and R. C. Pooser, Quantum sensing with squeezed light, ACS Photonics **6**, 1307 (2019).
[24] J. Abadie *et al.* (LIGO Scientific Collaboration), A gravitational wave observatory operating beyond the quantum shot-noise limit, Nat. Phys. **7**, 962 (2011).
[25] J. Aasi *et al.*, Enhanced sensitivity of the LIGO gravitational wave detector by using squeezed states of light, Nat. Photonics **7**, 613 (2013).
[26] H. Grote, K. Danzmann, K. L. Dooley, R. Schnabel, J. Slutsky, and H. Vahlbruch, First long-term application of squeezed states of light in a gravitational-wave observatory, Phys. Rev. Lett. **110**, 181101 (2013).
[27] K. Iwasawa, K. Makino, H. Yonezawa, M. Tsang, A. Davidovic, E. Huntington, and A. Furusawa, Quantum-limited mirror-motion estimation, Phys. Rev. Lett. **111**, 163602 (2013).
[28] V. Peano, H. G. L. Schwefel, Ch. Marquardt, and F. Marquardt, Intracavity squeezing can enhance quantum-limited optomechanical position detection through deamplification, Phys. Rev. Lett. **115**, 243603 (2015).
[29] N. Didier, J. Bourassa, and A. Blais, Fast quantum nondemolition readout by parametric modulation of longitudinal qubit-oscillator interaction, Phys. Rev. Lett. **115**, 203601 (2015).
[30] A. Eddins, S. Schreppler, D. M. Toyli, L. S. Martin, S. Hacohen-Gourgy, L. C. G. Govia, H. Ribeiro, A. A. Clerk, and I. Siddiqi, Stroboscopic qubit measurement with squeezed illumination, Phys. Rev. Lett. **120**, 040505 (2018).
[31] Sh. Barzanjeh, D. P. DiVincenzo, and B. M. Terhal, Dispersive qubit measurement by interferometry with parametric amplifiers, Phys. Rev. B **90**, 134515 (2014).
[32] N. Didier, A. Kamal, W. D. Oliver, A. Blais, and A. A. Clerk, Heisenberg-limited qubit read-out with two-mode squeezed light, Phys. Rev. Lett. **115**, 093604 (2015).
[33] L. C. G. Govia and A. A. Clerk, Enhanced qubit readout using locally generated squeezing and inbuilt Purcell-decay suppression, New J. Phys. **19**, 023044 (2017).
[34] G. Liu, X. Cao, T.-C. Chien, C. Zhou, P. Lu, and M. Hatridge, Noise reduction in qubit readout with a two-mode squeezed interferometer, Phys. Rev. Appl. **18**, 064092 (2022).
[35] A. Blais, A. L. Grimsmo, S. M. Girvin, and A. Wallraff, Circuit quantum electrodynamics, Rev. Mod. Phys. **93**, 025005 (2021).
[36] A. Wallraff, D. I. Schuster, A. Blais, L. Frunzio, J. Majer, M. H. Devoret, S. M. Girvin, and R. J. Schoelkopf, Approaching unit visibility for control of a superconducting qubit with dispersive readout, Phys. Rev. Lett. **95**, 060501 (2005).
[37] P. Krantz, A. Bengtsson, M. Simoen, S. Gustavsson, V. Shumeiko, W. D. Oliver, C. M. Wilson, P. Delsing, and J. Bylander, Single-shot read-out of a superconducting qubit using a Josephson parametric oscillator, Nat. Commun. **7**, 11417 (2016).
[38] T. Walter *et al.*, Rapid high-fidelity single-shot dispersive readout of superconducting qubits, Phys. Rev. Appl. **7**, 054020 (2017).
[39] X. Wang, A. Miranowicz, and F. Nori, Ideal quantum nondemolition readout of a flux qubit without purcell limitations, Phys. Rev. Appl. **12**, 064037 (2019).
[40] A. Crippa *et al.*, Gate-reflectometry dispersive readout and coherent control of a spin qubit in silicon, Nat. Commun. **10**, 2776 (2019).
[41] R. Dassonneville *et al.*, Fast high-fidelity quantum nondemolition qubit readout via a nonperturbative cross-Kerr coupling, Phys. Rev. X **10**, 011045 (2020).
[42] P. Schindler, J. T. Barreiro, T. Monz, V. Nebendahl, D. Nigg, M. Chwalla, M. Hennrich, and R. Blatt, Experimental repetitive quantum error correction, Science **332**, 1059 (2011).
[43] J. Kelly *et al.*, State preservation by repetitive error detection in a superconducting quantum circuit, Nature (London) **519**, 66 (2015).
[44] S. Krinner *et al.*, Realizing repeated quantum error correction in a distance-three surface code, Nature (London) **605**, 669 (2022).
[45] R. Raussendorf and J. Harrington, Fault-tolerant quantum computation with high threshold in two dimensions, Phys. Rev. Lett. **98**, 190504 (2007).
[46] J. M. Gambetta, J. M. Chow, and M. Steffen, Building logical qubits in a superconducting quantum computing system, npj Quantum Inf. **3**, 2 (2017).
[47] See Supplemental Material at http://link.aps.org/supplemental/10.1103/PhysRevLett.133.233605, which includes Refs. [48,49], for technical details of DQR in the cases of using IES and ICS separately and together, a detailed analysis of the qubit-cavity dispersive coupling enhanced by squeezing, and more discussions of the effects of parameter mismatches in realistic experiments on our readout proposal.
[48] I. Strandberg, G. Johansson, and F. Quijandría, Wigner negativity in the steady-state output of a Kerr parametric oscillator, Phys. Rev. Res. **3**, 023041 (2021).
[49] Y. Lu, I. Strandberg, F. Quijandría, G. Johansson, S. Gasparinetti, and P. Delsing, Propagating Wigner-negative states generated from the steady-state emission of a superconducting qubit, Phys. Rev. Lett. **126**, 253602 (2021).

[50] C.-F. Kam and X. Hu, Submicrosecond high-fidelity dispersive readout of a spin qubit with squeezed photons, Phys. Rev. A **109**, L040402 (2024).
[51] K. W. Murch, S. J. Weber, K. M. Beck, E. Ginossar, and I. Siddiqi, Reduction of the radiative decay of atomic coherence in squeezed vacuum, Nature (London) **499**, 62 (2013).
[52] H. Vahlbruch, D. Wilken, M. Mehmet, and B. Willke, Laser power stabilization beyond the shot noise limit using squeezed light, Phys. Rev. Lett. **121**, 173601 (2018).
[53] M. Malnou, D. A. Palken, B. M. Brubaker, L. R. Vale, G. C. Hilton, and K. W. Lehnert, Squeezed vacuum used to accelerate the search for a weak classical signal, Phys. Rev. X **9**, 021023 (2019).
[54] Y. Xia, A. R. Agrawal, C. M. Pluchar, A. J. Brady, Z. Liu, Q. Zhuang, D. J. Wilson, and Z. Zhang, Entanglement-enhanced optomechanical sensing, Nat. Photonics **17**, 470 (2023).
[55] M. Bartkowiak, L.-A. Wu, and A. Miranowicz, Quantum circuits for amplification of Kerr nonlinearity via quadrature squeezing, J. Phys. B **47**, 145501 (2014).
[56] S. Zeytinoğlu, A. İmamoğlu, and S. Huber, Engineering matter interactions using squeezed vacuum, Phys. Rev. X **7**, 021041 (2017).
[57] M.-A. Lemonde, N. Didier, and A. A. Clerk, Enhanced nonlinear interactions in quantum optomechanics via mechanical amplification, Nat. Commun. **7**, 11338 (2016).
[58] P.-B. Li, Y. Zhou, W.-B. Gao, and F. Nori, Enhancing spin-phonon and spin-spin interactions using linear resources in a hybrid quantum system, Phys. Rev. Lett. **125**, 153602 (2020).
[59] C. Zhong, M. Xu, A. Clerk, H. X. Tang, and L. Jiang, Quantum transduction is enhanced by single mode squeezing operators, Phys. Rev. Res. **4**, L042013 (2022).
[60] Y.-H. Chen, W. Qin, X. Wang, A. Miranowicz, and F. Nori, Shortcuts to adiabaticity for the quantum Rabi model: Efficient generation of giant entangled cat states via parametric amplification, Phys. Rev. Lett. **126**, 023602 (2021).
[61] C. Sánchez Muñoz and D. Jaksch, Squeezed lasing, Phys. Rev. Lett. **127**, 183603 (2021).
[62] L. Tang, J. Tang, M. Chen, F. Nori, M. Xiao, and K. Xia, Quantum squeezing induced optical nonreciprocity, Phys. Rev. Lett. **128**, 083604 (2022).
[63] O. Gamel and D. F. V. James, Time-averaged quantum dynamics and the validity of the effective Hamiltonian model, Phys. Rev. A **82**, 052106 (2010).
[64] A. Blais, R.-S. Huang, A. Wallraff, S. M. Girvin, and R. J. Schoelkopf, Cavity quantum electrodynamics for superconducting electrical circuits: An architecture for quantum computation, Phys. Rev. A **69**, 062320 (2004).
[65] T. Yamamoto, K. Inomata, M. Watanabe, K. Matsuba, T. Miyazaki, W. D. Oliver, Y. Nakamura, and J. S. Tsai, Flux-driven Josephson parametric amplifier, Appl. Phys. Lett. **93**, 042510 (2008).
[66] C.-F. Kam and X. Hu, Fast and high-fidelity dispersive readout of a spin qubit via squeezing and resonator nonlinearity, arXiv:2401.03617.